Selected Papers

Formation of Hierarchically Porous Hollow Spheres Composed of Dehydroxylated Imogolite and Carbonaceous Materials

Yoshiyuki Kuroda[1] **and Kazuyuki Kuroda***[1,2]

[1]Department of Applied Chemistry, Faculty of Science and Engineering, Waseda University, 3-4-1 Ohkubo, Shinjuku-ku, Tokyo 169-8555

[2]Kagami Memorial Research Institute for Materials Science and Technology, Waseda University, 2-8-26 Nishiwaseda, Shinjuku-ku, Tokyo 169-0051

Received September 16, 2010
E-mail: kuroda@waseda.jp

Hierarchically porous hollow spheres composed of dehydroxylated imogolite and carbonaceous materials were formed by using polystyrene particles as templates. A large amount of polystyrene particles were removed by heat treatment at relatively low temperature, leaving a small amount of highly porous carbonaceous material and retaining micropores of imogolite nanotubes.

Hierarchically porous materials are of great importance because of their potential applications in catalysis, separation, and devices,[1] owing to their high surface area, efficient diffusion of guest species, and tailored morphology. A colloidal templating technique is one of the most useful methods to fabricate three-dimensionally ordered macroporous[2] and hollow spherical[3] structures in hierarchically porous materials. Colloidal particles, consisting of polymers, silicates, and salts, have been utilized as templates for this technique.

Formation of hierarchically porous materials with multiple components is useful to integrate various properties into their frameworks. Templates can also be used as the sources of parts of frameworks if the removal conditions are finely tuned. For example, Polarz et al. have reported that mesoporous silica–carbon composite materials are promising as solar absorbers.[4] Consequently, carbonization of polymer templates is expected to provide hydrophobic porous carbons in the frameworks of hierarchically porous materials.

To fabricate hierarchically porous materials, we have focused on imogolite as a building block.[5] Imogolite is a hydrophilic microporous aluminosilicate nanotube (general composition: $Al_2SiO_3(OH)_4$) whose inner and outer diameters are ca. 1 and ca. 2 nm, respectively.[6] We have reported that positively charged imogolite nanotubes can be assembled with polyelectrolytes on polystyrene (PS) particles by a layer-by-layer technique to form core–shell structures.[5b] The core–shell particles are transformed into hierarchically porous hollow spheres composed mostly of dehydroxylated imogolite by heat treatment at 500 °C under an ambient atmosphere. If PS particles are carbonized, it is expected that hierarchically porous materials composed of both hydrophilic dehydroxylated imogolite and hydrophobic porous carbonaceous materials are formed. However, the heat treatment at high temperatures (700–900 °C) under an inert atmosphere is necessary for the carbonization of PS particles, which inevitably destroys the microporous structure of imogolite.[7]

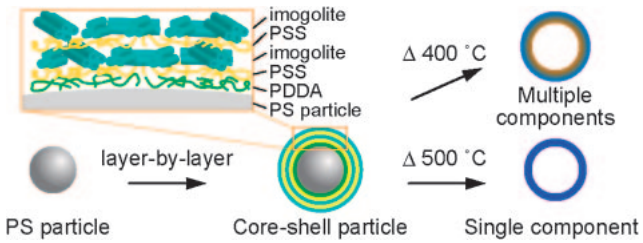

Scheme 1. Preparation of hierarchically porous hollow spheres at different heat treatment temperatures [PDDA: poly(diallyldimethylammonium chloride), PSS: poly(sodium 4-styrenesulfonate)].

In this paper, we have focused on the partial carbonization of PS at relatively low temperature under an ambient atmosphere.[8] The composition of the products was controlled by the temperature of the heat treatment (Scheme 1). We found that highly porous carbonaceous materials are formed on the hollow shells, retaining micropores of imogolite nanotubes. The present method is promising for the formation of hierarchically porous materials consisting of multiple components.

PS particles coated with multilayer shells composed of imogolite nanotubes and polyelectrolytes were prepared according to our report.[5b] Imogolite was synthesized according to the literature.[6,9,10] Poly(diallyldimethylammonium chloride) (PDDA, $M_w = 100000$–200000, Sigma-Aldrich Co.) and poly(sodium 4-styrenesulfonate) (PSS, $M_w = 70000$, Sigma-Aldrich Co.) were used as polycation and polyanion, respectively. PS particles ca. 850 nm in diameter (Seradyn Inc.) were coated layer-by-layer with multilayer shells consisting of PDDA(/PSS/imogolite)$_2$ (denoted as core–shell particles). The number of PSS/imogolite bilayers is smaller than that reported previously,[5b] which is better to increase the amount of carbonaceous materials relative to imogolite. The core–shell particles were thermally treated at 400 or 500 °C for 3 h under ambient conditions (denoted as H400 and H500, respectively).

Thermogravimetry-differential thermal analysis (TG-DTA) curves were recorded on a Rigaku TG8020 instrument with a heating rate of 5 °C min^{-1} under a dry air flow. Transmission electron microscopy (TEM) images were recorded with a JEOL JEM-2010 microscope with accelerating voltage at 200 kV. Carbon contents were determined by CHN analysis using a Perkin-Elmer PE-2400II apparatus. Energy dispersive X-ray (EDX) mapping data were recorded on a JEOL JEM-6500F microscope equipped with a JEOL JED-2300T spectrometer. The Fourier transform infrared (FTIR) spectra were recorded on a Perkin-Elmer Spectrum One spectrometer using a KBr disc. Powder X-ray diffraction (XRD) patterns were obtained with a Rigaku Ultima-III diffractometer using Cu Kα radiation (40 kV,

Published on the web December 18, 2010; doi:10.1246/bcsj.20100265

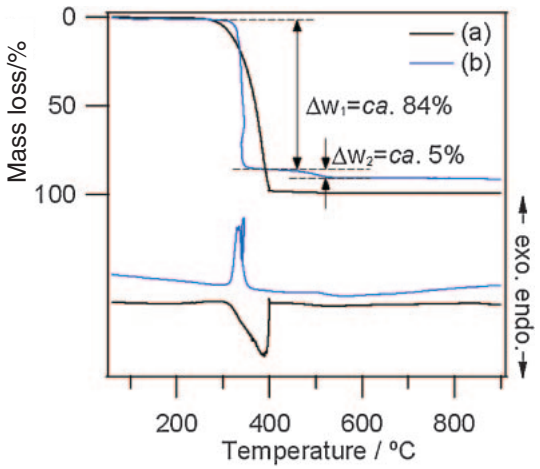

Figure 1. TG-DTA curves of (a) PS particles (sample amount: 1.79 mg) and (b) core–shell particles (1.19 mg) under a dry air flow.

40 mA). N_2 adsorption–desorption isotherms were measured with a Quantachrome Autosorb-1 apparatus.

The TG-DTA curves of bare PS particles show a mass loss with both endothermic and exothermic DTA peaks. These peaks indicate that PS particles are oxidatively decomposed (combusted) above 260 °C (extrapolated beginning temperature).[8] The following endothermic peak suggests that the combustion of PS particles is accompanied with carbon–carbon bond scission. The TG-DTA curves of core–shell particles show two-step mass losses with large exothermic DTA peaks above 320 °C and a small exothermic one above 430 °C (Figure 1). The results indicate that the combustion of PS particles became dominant in the core–shell particles and the residue formed by the first reaction was combusted at higher temperature. Because large and small mass losses occur at ca. 320 and ca. 430 °C, respectively, the core–shell particles were heat treated at 400 and 500 °C.

The color of core–shell particles (white) turned to brown when the particles were heat treated at 400 °C, whereas it became white again at 500 °C (Figures 2a and 2b). Both H400 and H500 are hollow spheres, which supports that PS particles are mostly removed by the heat treatment even at 400 °C (Figures 2c and 2d). The carbon contents in H400 and H500 estimated by CHN analyses were 19 and 0.5 wt %, respectively. Therefore, the brown color is probably due to incompletely decomposed residue of PS particles. The EDX mapping also shows that carbons are located on hollow spheres (Figure S1). Though carbonaceous residues were not well observed from the TEM image (Figure 2c), they should reside on the inner surface and inside the shells of hollow spheres.

The FTIR spectrum of core–shell particles shows many absorption bands due to PS particles and polyelectrolytes (the assignments are described elsewhere,[5b] Figure 3a). Even though 19 wt % of carbon is present in H400, its FTIR spectrum shows almost no bands due to organic components (Figure 3b). Therefore, the carbon contents correspond mostly to carbonaceous materials. The bands at ca. 1400 and ca. 1700 cm^{-1} may be attributable to C–OH stretching and C=O stretching vibrations[11] of partially oxidized carbonaceous materials. The bands at 400–800 and 900–1200 cm^{-1} are

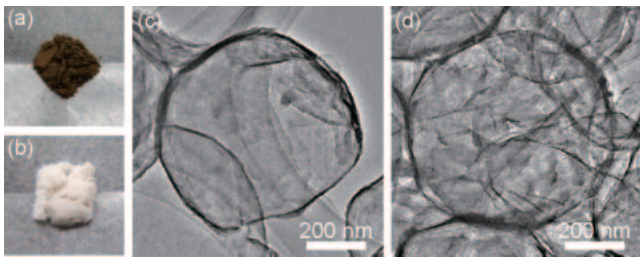

Figure 2. Photographs of (a) H400 and (b) H500 and (c, d) their TEM images, respectively.

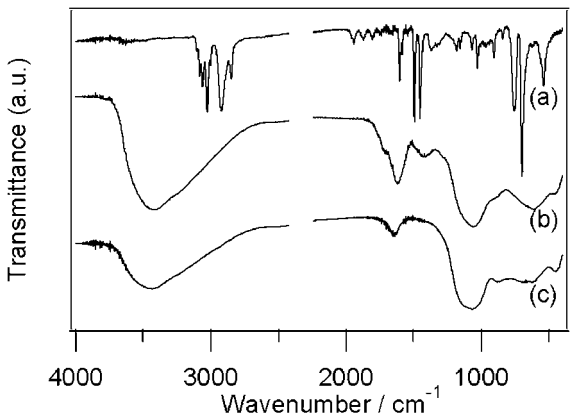

Figure 3. FTIR spectra of (a) core–shell particles, (b) H400, and (c) H500.

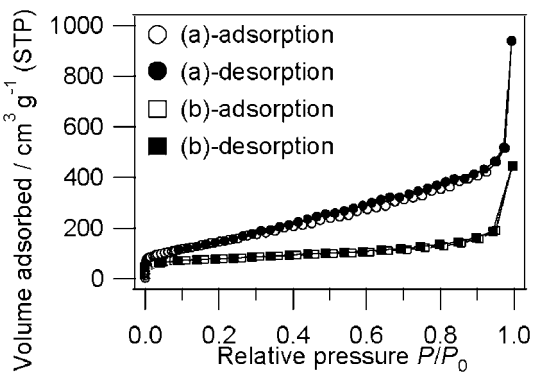

Figure 4. N_2 adsorption–desorption isotherms of (a) H400 and (b) H500.

attributable to dehydroxylated imogolite with amorphous structure.[7] The spectrum of H500 shows absorption bands only due to dehydroxylated imogolite (Figure 3c). From these data, it is reasonable to estimate that H400 consists of dehydroxylated imogolite and amorphous carbonaceous materials and that H500 consists of only dehydroxylated imogolite. The XRD patterns of both H400 and H500, indicating only broad peaks due to amorphous materials (Figure S2), are consistent with this estimate.

The N_2 adsorption–desorption isotherm of H400 shows a noticeable difference from that of H500 (Figure 4). The BET surface area of H400 (ca. 500 $m^2 g^{-1}$) is much higher than that of H500 (ca. 290 $m^2 g^{-1}$). This high value of H400 is not explained only by the presence of imogolite (The highest BET surface area of imogolite is 398 $m^2 g^{-1}$ when heat treated at 275 °C).[12] Consequently, the amorphous carbonaceous materi-

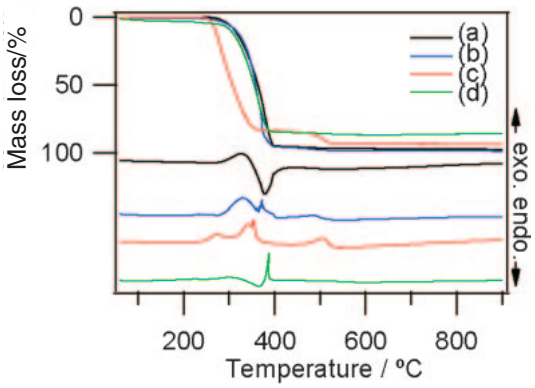

Figure 5. TG-DTA curves of PS particles coated with (a) PDDA (sample amount: 4.53 mg), (b) PDDA/PSS (6.59 mg), and (c) imogolite (3.21 mg) and (d) a physical mixture of PS particles and imogolite (2.97 mg).

als certainly contribute to its high porosity. The uptake at $P/P_0 < 0.1$ is due to the adsorption in the intratubular micropores of imogolite, showing little structural difference in micropores between H400 and H500. At $0.1 < P/P_0 < 0.9$, the gradual increase in the adsorption amount was observed only for H400. Thus, additional widely distributed mesopores (2–8 nm, Figure S3) are attributable mainly to amorphous carbonaceous materials formed only in H400. The steep uptake at $P/P_0 > 0.9$ is due to adsorption in macropores, which are thought to be inside or among hollow spheres. Therefore, H400 possesses micro–meso–macro hierarchical porosity due to both dehydroxylated imogolite and amorphous carbonaceous materials.

The change in the decomposition behavior of PS particles is caused by their confinement in multilayer shells composed of imogolite nanotubes and/or polyelectrolytes. The DTA curve of PS particles coated only with PDDA shows a small exothermic peak and a large endothermic peak (Figure 5a). That of PS particles coated with PDDA/PSS shows only exothermic peaks due to the combustion of PS particles (Figure 5b). These results suggest that the oxidative decomposition becomes more dominant when the PS particles are confined in thicker multilayer shells even though they are organic. The DTA curve of PS particles coated only with imogolite also shows obvious exothermic peaks (Figure 5c and Supporting Information), which indicates that the thermal decomposition behavior changes more significantly when PS particles are confined in the layer of imogolite. In this case, more carbonaceous materials remained than in the case of H400, whereas such core–shell particles with monolayer of imogolite cannot retain their hollow spherical structures.[5b] When a physical mixture of PS particles (80 wt %) and imogolite (20 wt %) was used, the TG-DTA curves are similar to those of bare PS particles (Figure 5d and Supporting Information). Therefore, the influence of imogolite for the decomposition behavior is considerably enhanced when PS particles are coated with the shells. Therefore, the role of imogolite nanotubes is not only to provide micropores but also to enhance partial carbonization of PS particles. The reasons for such changes are possibly related to the catalytic activity of inorganic surfaces for oxidation of polymers[13] or limited diffusion of decomposed products in the confined spaces,[14] though further studies are needed to clarify the confinement effect.

In conclusion, hierarchically porous hollow spheres composed of dehydroxylated imogolite and carbonaceous materials were formed by using PS particles as both templates and carbon sources. A large amount of PS particles were removed by heat treatment at 400 °C, leaving a small amount of highly porous carbonaceous materials and retaining micropores of imogolite nanotubes. Imogolite is found to be useful as a microporous building block and to change thermal decomposition behavior of PS particles to improve functionalities of hierarchically porous materials.

This work was supported by the Elements Science and Technology Project "Functional Designs of Silicon-Oxygen-Based Compounds by Precise Synthetic Strategies" and the Global COE program "Practical Chemical Wisdom" from MEXT, Japan. Y. K. is grateful for financial support via a Grant-in-Aid for the Japan Society for the Promotion of Science (JSPS) Fellows from MEXT.

Supporting Information

EDX mapping (Figure S1), XRD patterns (Figure S2), BJH pore size distribution (Figure S3), and the experimental procedures are available free of charge on the web at http://www.csj.jp/journals/bcsj/.

References

1 a) J. Pérez-Ramírez, C. H. Christensen, K. Egeblad, C. H. Christensen, J. C. Groen, *Chem. Soc. Rev.* **2008**, *37*, 2530. b) K. Nakanishi, N. Tanaka, *Acc. Chem. Res.* **2007**, *40*, 863. c) I. Soten, G. A. Ozin, *Curr. Opin. Colloid Interface Sci.* **1999**, *4*, 325.

2 A. Stein, F. Li, N. R. Denny, *Chem. Mater.* **2008**, *20*, 649.

3 a) F. Caruso, R. A. Caruso, H. Möhwald, *Science* **1998**, *282*, 1111. b) J. Liu, F. Liu, K. Gao, J. Wu, D. Xue, *J. Mater. Chem.* **2009**, *19*, 6073.

4 Y. Mastai, S. Polarz, M. Antonietti, *Adv. Funct. Mater.* **2002**, *12*, 197.

5 a) Y. Kuroda, M. Tamakoshi, J. Murakami, K. Kuroda, *J. Ceram. Soc. Jpn.* **2007**, *115*, 233. b) Y. Kuroda, K. Kuroda, *Sci. Technol. Adv. Mater.* **2008**, *9*, 025018. c) N. Jiravanichanun, K. Yamamoto, H. Yonemura, S. Yamada, H. Otsuka, A. Takahara, *Bull. Chem. Soc. Jpn.* **2008**, *81*, 1663.

6 V. C. Farmer, M. J. Adams, A. R. Fraser, F. Palmieri, *Clay Miner.* **1983**, *18*, 459.

7 a) J. D. Russell, W. J. McHardy, A. R. Fraser, *Clay Miner.* **1969**, *8*, 87. b) D.-Y. Kang, J. Zang, E. R. Wright, A. L. McCanna, C. W. Jones, S. Nair, *ACS Nano* **2010**, *4*, 4897.

8 B. Martel, *J. Appl. Polym. Sci.* **1988**, *35*, 1213.

9 S.-I. Wada, *Nendo Kagaku* **1985**, *25*, 53.

10 M. Suzuki, F. Ohashi, K. Inukai, M. Maeda, S. Tomura, *Nendo Kagaku* **2000**, *40*, 1.

11 G. Socrates, *Infrared and Raman Characteristic Group Frequencies: Tables and Charts*, 3rd ed., Wiley, New York, **2004**.

12 W. C. Ackerman, D. M. Smith, J. C. Huling, Y.-W. Kim, J. K. Bailey, C. J. Brinker, *Langmuir* **1993**, *9*, 1051.

13 H. Qin, S. Zhang, C. Zhao, M. Feng, M. Yang, Z. Shu, S. Yang, *Polym. Degrad. Stab.* **2004**, *85*, 807.

14 T. Kato, H. Ushijima, M. Katsumata, T. Hyodo, Y. Shimizu, M. Egashira, *J. Am. Ceram. Soc.* **2004**, *87*, 60.